Differentiation and Passivity for Control of Brayton-Moser Systems

Krishna Chaitanya Kosaraju, Michele Cucuzzella, Jacquelien M. A. Scherpen and Ramkrishna Pasumarthy

Abstract—This paper deals with a class of Resistive-Inductive-Capacitive (RLC) circuits and switched RLC (s–RLC) circuits modeled in the Brayton Moser framework. For this class of systems, new passivity properties using a Krasovskii-type Lyapunov function as storage function are presented, where the supply-rate is function of the system states, inputs and their first time derivatives. Moreover, after showing the integrability property of the port-variables, two *simple* control methodologies called *output shaping* and *input shaping* are proposed for regulating the voltage in RLC and s–RLC circuits. Global asymptotic stability is theoretically proved for both the proposed control methodologies. Moreover, robustness with respect to load uncertainty is ensured by the *input shaping* methodology. The applicability of the proposed methodologies is illustrated by designing voltage controllers for DC-DC converters and DC networks.

Index Terms—Brayton-Moser systems, passivity-based control, RLC circuits, power converters, DC networks.

I. INTRODUCTION

In the recent years, passivity theory has gained renewed attention because of its advantages and practicality in modeling and control of multi-domain dynamical systems [1], [2]. In general, a system is passive if there exists a (bounded from below) *storage function* $S : \mathbb{R}^n \to \mathbb{R}_+$ satisfying

$$S(x(t)) - S(x(0)) \leq \int_0^t u^\top y dt, \tag{1}$$

where $x \in \mathbb{R}^n$ is the system state, $u, y \in \mathbb{R}^m$ are the input and the output, also called *port-variables* and the product $u^\top y$ is commonly known as *supply-rate* [3], [4]. Naturally, one can interpret the storage function as the total system energy, and the supply rate as the power supplied to the system. Consequently, inequality (1) implies that the newly *stored* energy is never greater than the *supplied* one.

In order to analyze the passivity properties of a general nonlinear system, it is usually required to be artful in designing the storage function. For this reason, it is helpful to recast the system dynamics into a known framework, such as the port-Hamiltonian (pH) one [5], where the storage function, also called Hamiltonian function, generally depends on the

K. C. kosaraju is with Department of Electrical Engineering, University of Notre Dame, 275 Fitzpatrick Hl Engrng, Notre Dame, IN 46556, USA.

M. Cucuzzella and J. M. A. Scherpen are with the Jan C. Wilems Center for Systems and Control, ENTEG, Faculty of Science and Engineering, University of Groningen, Nijenborgh 4, 9747 AG Groningen, the Netherlands.

R. Pasumarthy is with Department of electrical engineering, Indian Institute of Technology-Madras, Chennai-36, India. (email: k.c.kosaraju@nd.edu, {m.cucuzzella, j.m.a.scherpen}@rug.nl, ramkrishna@ee.iitm.ac.in)

system energy. Another well known framework that has been extensively explored for modeling of nonlinear Resistive-Inductive-Capacitive (RLC) circuits, is the Brayton-Moser (BM) framework [6], [7], where the storage function relies on the system power (see [8] for further details on geometric modeling of nonlinear RLC circuits).

Nowadays, power-converters play a prominent role in smart grids. Conventional power-converters consist of (passive) sub-systems interconnected through switches. In this paper, we consider a large class of *switched* RLC (s–RLC) circuits, which models the majority of the existing power converters (e.g., buck, boost, buck-boost and Cúk). Although the analysis of s–RLC circuits has received a significant amount of attention (see for instance [9]–[12] and the references therein), we notice that results based on the *passivity properties* of the open-loop system are still lacking. On the other hand, a significant number of results have been published relying on Passivity-Based Control (PBC) [13]–[19], where the main idea is generally to passify the controlled system such that the closed-loop storage function has a minimum at the desired operating point [2]. However, the passivity properties and the control techniques developed for pH systems cannot be straightforwardly applied to s–RLC networks. Alternatively, in [20] the authors formalize the use of the BM framework for analyzing s–RLC circuits and also provide tuning rules based on the well-known BM theorems.

A. Motivation and Main Contributions

Lyapunov theory is fundamental in systems theory. In order to study the stability of a dynamical system, one generally needs to find a suitable Lyapunov function. Krasovskii proposed a simple and elegant candidate Lyapunov function, where one needs to compute some point-wise conditions for sufficiency of Lyapunov stability [21]. In a similar manner, passivity theory hinges on finding candidate storage functions satisfying (1). However, the candidate Lyapunov function proposed by Krasovskii is not well explored as a storage function. In [22]–[24], the authors presented a preliminary result on the passivity property for a class of RLC circuits using such a storage function, named *Krasovskii storage function*, i.e.,

$$S(x, \dot{x}) = \frac{1}{2} \dot{x}^\top M(x) \dot{x}, \tag{2}$$

where $M(x) > 0 \in \mathbb{R}^{n \times n}$. By using such a storage function, in this paper we present completely new passivity properties

with inductors. In [6], [7], Brayton and Moser show that the dynamics‡ of this class of systems can be represented as

$$-L\dot{I} = \nabla_I P(I,V) - Bu_s$$
$$C\dot{V} = \nabla_V P(I,V), \tag{3}$$

where $L \in \mathbb{R}^{\sigma \times \sigma}$ and $C \in \mathbb{R}^{\rho \times \rho}$ are the inductances and capacitances matrices, respectively. The state variables $I \in \mathbb{R}^{\sigma}$ and $V \in \mathbb{R}^{\rho}$ denote the currents through the σ inductors and the voltages across the ρ capacitors, respectively. The matrix $B \in \mathbb{R}^{\sigma \times m}$ is the input matrix with full column rank and $P : \mathbb{R}^{\sigma \times \rho} \to \mathbb{R}$ represents the so-called *mixed-potential* function, given by,

$$P(I,V) = I^\top \Gamma V + P_R(I) - P_G(V), \tag{4}$$

where $\Gamma \in \mathbb{R}^{\sigma \times \rho}$ captures the power circulating across the dynamic elements. The resistive content $P_R : \mathbb{R}^{\sigma} \to \mathbb{R}$ and the resistive co-content $P_G : \mathbb{R}^{\rho} \to \mathbb{R}$ capture the power dissipated in the resistors connected in series to the inductors and in parallel to the capacitors, respectively.

Remark 1 (Current sources). *For the sake of simplicity, in* (3) *we have not included current sources. However, the results presented in this note can also be developed for current sources in a straightforward manner.*

According to the BM formulation, system (3) can compactly be written as

$$Q\dot{x} = \nabla_x P(x) + \tilde{B}u_s, \tag{5}$$

where $x = (I^\top, \; V^\top)^\top$, $Q = \text{diag}\{-L, C\}$ and $\tilde{B} = (-B^\top \; O)^\top$, $O \in \mathbb{R}^{m \times \rho}$ being a zero-matrix. To permit the controller design in the following sections, we introduce the following assumptions:

Assumption 1 (Inductance and capacitance matrices). *Matrices L and C are constant, symmetric§ and positive-definite.*

Assumption 2 (Resistive content and co-content). *The resistive content and co-content of current controlled resistors R and voltage controlled resistors G are quadratic in I and V respectively, i.e.,*

$$P_R(I) = \frac{1}{2}I^\top R I, \qquad P_G(V) = \frac{1}{2}V^\top G V, \tag{6}$$

where $R \in \mathbb{R}^{\sigma \times \sigma}$ and $G \in \mathbb{R}^{\rho \times \rho}$ are positive semi-definite matrices.

Under Assumptions 1 and 2, it can be shown that system (3) is passive with respect to the *power-conjugate*¶ port-variables u_s, $B^\top I$ and the total energy stored in the network as storage function (see Remark 3).

‡For further details and a large number of examples, we suggest the reading of the sidebar 'History of the Mixed-Potential Function' and section 'The Brayton-Moser equations' in [1].
§Matrices L and C can possibly capture mutual inductances and capacitances, respectively.
¶We use the expression *power-conjugate* to indicate that the product of input and output has units of power.

Table I
DESCRIPTION OF THE USED SYMBOLS

	State variables
I	Inductor current
V	Capacitor voltage
	Parameters
L	Inductance
C	Capacitance
G	Conductance
R	Resistance
	Inputs
u_s	Control input (RLC circuits)
u	Duty cycle (s–RLC circuits)
V_s	Voltage source (s–RLC circuits)

B. (Average) Switched Electrical Circuits

We now consider the class of RLC circuits including an ideal switch‖ (s–RLC). Let $u_d \in \{0,1\}$ and $V_s \in \mathbb{R}^m$ denote the state of the switching element, i.e., *open* or *closed*, and the (current-controlled) voltage sources, respectively. To describe the dynamics of s–RLC circuits we adopt the BM formulation (3) with the mixed-potential function and input matrix depending on the state of the switching element, i.e., $P : \{0,1\} \times \mathbb{R}^{\sigma} \times \mathbb{R}^{\rho} \to \mathbb{R}$ and $B : \{0,1\} \to \mathbb{R}^{\sigma \times m}$ can be expressed as

$$P(u_d, I, V) = u_d P_1(I,V) + (1-u_d)P_0(I,V)$$
$$B(u_d) = u_d B_1 + (1-u_d)B_0, \tag{7}$$

where $P_1(I,V)$, B_1 and $P_0(I,V)$, B_0 represent the mixed-potential function and the input matrix of the s–RLC circuit when $u_d = 1$ and $u_d = 0$, respectively. Under the reasonable assumption that the Pulse Width Modulation (PWM) frequency is sufficiently high, the state of the system can be replaced by the corresponding average state representing the average inductor currents and capacitor voltages, while the switching control input is replaced by the so called duty cycle of the converter [10]. For the sake of notational simplicity, from now let I, V and $u \in [0,1]$ denote the average signals of I, V and u_d, respectively, throughout the rest of the paper. Consequently, the average behaviour of a s–RLC electrical circuit can be represented by the following BM equations

$$-L\dot{I} = \nabla_I P(u,I,V) - B(u)V_s$$
$$C\dot{V} = \nabla_V P(u,I,V). \tag{8}$$

Remark 2 (Resistive content and co-content structure). *Note that if the content and co-content structure is not affected by the switching signal, the mixed-potential function in* (7) *can be rewritten as follows*

$$P(u,I,V) = I^\top \Gamma(u)V + P_R(I) - P_G(V), \tag{9}$$

where the mapping $\Gamma : [0,1] \to \mathbb{R}^{\sigma \times \rho}$ is defined as

$$\Gamma(u) = u\Gamma_1 + (1-u)\Gamma_0, \tag{10}$$

‖For the sake of simplicity we restrict the analysis to RLC circuits including only one switch. However, in Section IV-C we analyze a DC network including an arbitrary number of switches.

and Γ_1, Γ_0 *capture the interconnection of the storage elements (i.e., inductors and capacitors) when* $u = 1$ *and* $u = 0$, *respectively.*

In the following we consider that the resistive content and co-content structure is not affected by the switching signal. As a consequence, system (8) can be written as

$$-L\dot{I} = RI + \Gamma(u)V - B(u)V_s$$
$$C\dot{V} = \Gamma^\top(u)I - GV. \tag{11}$$

The main symbols used in (3)–(11) are described in Table I.

Remark 3 (Total energy as storage function). *It can be shown that the RLC circuit* (3) *is passive with respect to the storage function*

$$S_e(I, V) = \frac{1}{2}I^\top LI + \frac{1}{2}V^\top CV, \tag{12}$$

and port-variables u_s *and* $B^\top I$ *(see for instance [2]). Consider now the s–RLC circuit* (11)*. The first time derivative of the storage function* (12) *along the solutions to* (11) *satisfies*

$$\dot{S}_e \le I^\top B_0 V_s + uI^\top (B_1 - B_0) V_s.$$

Consequently, system (11) *is passive with respect to the storage function* (12) *and supply rate* $uI^\top B_1 V_s$ *if and only if* $B_0 = 0$ *and* $B_1 \ne 0$. *However, if we consider for instance the model of the boost converter (see Section IV-B), the conditions* $B_0 = 0$ *and* $B_1 \ne 0$ *are not satisfied. Furthermore, even supposing that the conditions* $B_0 = 0$ *and* $B_1 \ne 0$ *hold, we notice that the supply rate* $uI^\top B_1 V_s$ *is generally not equal to zero at the desired operating point, implying the occurrence of the so-called 'dissipation obstacle' problem [2].*

As a consequence of Remark 3, adopting the pH framework (using the total energy as Hamiltonian) does not provide any additional advantage compared to the BM framework. Moreover, s–RLC circuits do not inherit a standard pH structure [10]:

Remark 4 (Port-Hamiltonian formulation for s–RLC circuits). *Generally, a standard port-Hamiltonian system has the following structure*

$$\dot{x} = [J(x) - R(x)]\nabla_x H(x) + g(x)u, \tag{13}$$

where $x : \mathbb{R}_+ \to \mathbb{R}^n$, $u : \mathbb{R}_+ \to \mathbb{R}^m$ *denote the state and input, respectively,* $J(x) = -J(x)^\top$, $R(x) \ge 0$, $H : \mathbb{R}^n \to \mathbb{R}_+$ *is the Hamiltonian and* $g(x)$ *the input matrix. The skew symmetric matrix* $J(x)$ *generally captures the interconnection of the storage elements and* $R(x)$ *describes the dissipation structure of the system. As a result we have the following dissipation inequality:*

$$\dot{H} \le u^\top y,$$

where $y = g(x)^\top \nabla_x H(x)$. *However, s–RLC circuit do not generally inherit this structure. To represent s–RLC circuits it may be needed to modify* (13) *as follows (see [10] for some examples):*

$$\dot{x} = [J(x, u) - R(x)] \nabla_x H(x) + g(x)V_s, \tag{14}$$

where $J(x, u) = J_0(x) + \sum_{i=1}^{m} J_i(x)u_i$, $J_i + J_i^\top = 0$ *for all* $i \in \{0, \dots, m\}$, u *and* V_s *denote the duty-ratio and the supply voltage, respectively. This implies the following dissipation inequality:*

$$\dot{H} \le V_s^\top y, \tag{15}$$

which may be not useful for control purpose, since V_s *is generally not controllable.*

Alternatively, in [25, Theorem 1] it is shown, under some assumptions, that system (3) is passive with respect to the port-variables u_s, $B^\top \dot{I}$ and the so-called *transformed* mixed-potential function as storage function. However, finding the transformed mixed-potential function is not trivial and often requires that (sufficient) conditions on the system parameters are satisfied. Differently, in this work we overcome these issues by proposing a Krasovkii's Lyapunov function similar to (2) as storage function.

C. Problem Formulation

The main goal of this paper is to propose new passivity-based control methodologies for regulating the voltage in RLC and s–RLC circuits.

Before formulating the control objective and in order to permit the controllers design in the next sections, we first make the following assumption on the available information about systems (3) and (11):

Assumption 3 (Available information). *The state variables* I *and* V *are measurable*[**]. *The voltage source* V_s *in* (11) *is known and different from zero.*

Secondly, in order to formulate the control objective aiming at voltage regulation, we introduce the following two assumptions on the existence of a desired reference voltage for both RLC and s–RLC circuits, respectively:

Assumption 4 (Feasibility for RLC circuits). *There exist a constant desired reference voltage* $V^\star \in \mathbb{R}_+^\rho$ *and a constant control input* $\overline{u}_s$ *such that a steady state solution* $(\overline{I}, V^\star)$ *to system* (3) *satisfies*

$$0 = \Gamma V^\star + R\overline{I} - B\overline{u}_s$$
$$0 = \Gamma^\top \overline{I} - GV^\star. \tag{16}$$

Assumption 5 (Feasibility for s–RLC circuits). *There exist a constant desired reference voltage* $V^\star \in \mathbb{R}_+^\rho$ *and a constant control input* $\overline{u} \in (0, 1)$ *such that a steady state solution* $(\overline{I}, V^\star)$ *to system* (11) *satisfies*

$$0 = \Gamma(\overline{u})V^\star + R\overline{I} - B(\overline{u})V_s$$
$$0 = \Gamma^\top(\overline{u})\overline{I} - GV^\star. \tag{17}$$

We notice now that system (11) can be written as follows

$$\begin{bmatrix} -L\dot{I} \\ C\dot{V} \end{bmatrix} = \begin{bmatrix} RI + \Gamma_0 V - B_0 V_s \\ \Gamma_0^\top I - GV \end{bmatrix}$$
$$+ \begin{bmatrix} (\Gamma_1 - \Gamma_0) V - (B_1 - B_0) V_s \\ (\Gamma_1 - \Gamma_0)^\top I \end{bmatrix} u.$$

[**]Note that, when needed, we also assume that $\dot{I}$ and $\dot{V}$ are available.

Consequently, we introduce the following assumption for controllability purposes:

Assumption 6 (Controllability necessary condition). *There exists (at least) an element in the column vector*

$$\begin{bmatrix} (\Gamma_1 - \Gamma_0) V - (B_1 - B_0) V_s \\ (\Gamma_1 - \Gamma_0)^\top I \end{bmatrix}$$

that is different from zero for all $(I, V) \in \mathbb{R}^{\sigma \times \rho}$ and any $t \geq 0$.

The control objective can now be formulated explicitly:

Objective 1 (Voltage regulation).

$$\lim_{t \to \infty} V(t) = V^\star. \tag{18}$$

Remark 5 (Robustness to load uncertainty). *In power networks it is generally desired that Objective 1 is achieved independently from the load parameters, which are indeed often unknown (see also Assumption 3).*

III. The Proposed Control Approaches

In this section, we present new passivity properties (akin to differential passivity [38]) for the considered RLC circuits (3). Then, we extend these properties to s–RLC circuits (11).

A. New passivity properties

Novel passive maps for a class of RLC circuits are presented in [23][††], where the authors use a Krasovskii-type storage function similar to (2), i.e.,

$$S(\dot{I}, \dot{V}) = \frac{1}{2} \|\dot{I}\|_L^2 + \frac{1}{2} \|\dot{V}\|_C^2. \tag{19}$$

The use of such a storage function enables to relax the constraints on the system parameters required in [25, Theorem 1].

Since the storage function (19) depends on $\dot{I}$ and $\dot{V}$, we consider the following *extended-dynamics*[‡‡] of system (3)

$$-L\dot{I} = \Gamma V + RI - Bu_s \tag{20a}$$
$$C\dot{V} = \Gamma^\top I - GV \tag{20b}$$
$$-L\ddot{I} = \Gamma \dot{V} + R\dot{I} - B v_s \tag{20c}$$
$$C\ddot{V} = \Gamma^\top \dot{I} - G\dot{V} \tag{20d}$$
$$\dot{u}_s = v_s, \tag{20e}$$

where $(I, V, \dot{I}, \dot{V}, u_s)$ and $v_s \in \mathbb{R}^m$ are the (extended) system state and input, respectively. Then, inspired by [22]–[24], the following result can be established.

Proposition 1 (Passivity of RLC circuit). *Let Assumptions 1 and 2 hold. System (20) is passive with respect to the storage function (19) and the port-variables $y_s = B^\top \dot{I}$ and v_s.*

Proof. The first time derivative of the storage function (19) along the trajectories of (20) satisfies

$$\dot{S} \leq \dot{u}_s^\top B^\top \dot{I} = v_s^\top y_s. \tag{21}$$

[††]The class of RLC circuits considered in [23] is a sub-class of the systems analyzed in this paper. More precisely, in [23] the authors assume that L, C are diagonal and R, G are positive definite. These assumptions are relaxed in this paper (see Assumptions 1 and 2).

[‡‡]These dynamics are differentially extended with respect to time.

Remark 6. (**Physical interpretation of** (21)) *The established passivity property can be interpreted as the passivity property derived from the total energy of the 'dual' circuit, which is constructed by using capacitors as inductors, voltage sources as current sources and vice-versa. This follows from considering V_L as the voltage across the inductor and I_C as the current through the capacitor. As a consequence, the storage function (19) can be rewritten as*

$$S(I_C, V_L) = \frac{1}{2} \|V_L\|_{L^{-1}}^2 + \frac{1}{2} \|I_C\|_{C^{-1}}^2. \tag{22}$$

In (22), the term $1/2\|V_L\|_{L^{-1}}^2$ represents the energy stored into a capacitor with capacitance L^{-1} and charge $q_L = L^{-1} V_L$. Similarly, the term $1/2\|I_C\|_{C^{-1}}^2$ represents the energy stored into an inductor with inductance C^{-1} and flux $\phi_C = C^{-1} I_C$. Furthermore, let i_s denote the current source constructed from a capacitor with capacitance L^{-1} and charge $L^{-1} B u_s$. As a result, (21) becomes

$$\dot{S} \leq \dot{u}_s^\top B^\top L^{-1} V_L = i_s^\top V_L. \tag{23}$$

Before presenting an analogous passive map also for s–RLC circuits (11), similarly to (20) we consider the following extended dynamics of system (11)

$$-L\dot{I} = RI + \Gamma(u)V - B(u)V_s \tag{24a}$$
$$C\dot{V} = \Gamma^\top(u)I - GV \tag{24b}$$
$$-L\ddot{I} = R\dot{I} + \Gamma(u)\dot{V} + ((\Gamma_1 - \Gamma_0) V - (B_1 - B_0) V_s) v \tag{24c}$$
$$C\ddot{V} = \Gamma^\top(u)\dot{I} + (\Gamma_1 - \Gamma_0)^\top I v - G\dot{V} \tag{24d}$$
$$\dot{u} = v, \tag{24e}$$

where $(I, V, \dot{I}, \dot{V}, u)$ and $v \in \mathbb{R}$ are the (extended) system state and input, respectively. Then, the following result can be established.

Proposition 2 (Passivity of s–RLC circuit). *Let Assumptions 1 and 2 hold. System (24) is passive with respect to the storage function (19) and the port-variables v and*

$$y = \Big(\dot{V}^\top (\Gamma_1 - \Gamma_0)^\top I - \dot{I}^\top (\Gamma_1 - \Gamma_0) V \\ - \dot{I}^\top (B_0 - B_1) V_s \Big). \tag{25}$$

Proof. The time derivative of the storage function (19) along the trajectories of (24) satisfies

$$\begin{aligned} \dot{S} &= -\dot{I}^\top \Big(\big((1-u)\Gamma_0 + u\Gamma_1\big)\dot{V} + \dot{u}(\Gamma_1 - \Gamma_0)V \\ &\quad + R\dot{I} - \dot{u}(B_1 - B_0)V_s \Big) + \dot{V}^\top \Big(\big((1-u)\Gamma_0 \\ &\quad + u\Gamma_1\big)\dot{I} + \dot{u}(\Gamma_1 - \Gamma_0)^\top I - G\dot{V} \Big) \\ &= -\dot{I}^\top R \dot{I} - \dot{V}^\top G \dot{V} + \dot{u}y \\ &\leq \dot{u}y = vy. \end{aligned} \tag{26}$$

Note that, if V_s is controllable, then the storage function (19) along the extended dynamics of (11) satisfies

$$
\begin{aligned}
\dot{S} = & -\dot{I}^\top R \dot{I} - \dot{V}^\top G \dot{V} + \dot{u}y + \dot{I}^\top B(u)\dot{V}_s \\
& \le vy + \theta^\top \phi.
\end{aligned}
\tag{27}
$$

where $\theta = \dot{V}_s$ and $\phi = B(u)^\top \dot{I}$. Therefore the extended dynamics of (11) are passive with port variables $[v, \ \theta^\top]^\top$ and $[y, \ \phi^\top]^\top$.

Remark 7. (Insights on the storage function S) *The storage function (19) depends on the states $\dot{I}, \dot{V}$ of system (20) or (24). Consequently, S depends on the entire state of the extended system (20) or (24). This follows from replacing $\dot{I}, \dot{V}$ by the corresponding dynamics (20a)–(20b) or (24a)–(24b). Moreover, we will show in Theorems 3 and 4 that designing the controller by using the storage function (19) enables the achievement of Objective 1 despite the load uncertainty (see Remark 5). However, the cost of designing a robust controller is the need of information about the first time derivative of the signals I and V.*

By using the passive maps presented in Propositions 1 and 2, we propose in the next two subsections two different passivity-based control methodologies for both RLC and s–RLC circuits, respectively.

B. Output Shaping

The first methodology, which we call *output shaping*, relies on the integrability property of the *output* port-variable. More precisely, we use the integrated output port-variable to shape the closed-loop storage function. In this subsection, we first extend this methodology to a wider class of RLC circuits than the one considered in [23]. Subsequently, we further extend the output shaping methodology to s–RLC circuits.

Theorem 1 (Output shaping for RLC circuits)**.** *Let Assumptions 1–4 hold. Consider system (20) with control input v_s given by*

$$
v_s = \left(\mu_s - k_i B^\top \left(I - \bar{I} \right) - k_d y_s \right),
\tag{28}
$$

with $y_s = B^\top \dot{I}$, $k_d > 0$, $k_i > 0$ and $\mu_s \in \mathbb{R}^m$. The following statements hold:

(a) *System (20) in closed-loop with control (28) defines a passive map $\mu_s \mapsto y_s$.*
(b) *Let μ_s be equal to zero. If any of the following conditions holds*

  (i) *$R > 0$ and $G > 0$,*
  (ii) *$G > 0$ and $\Gamma^\top$ has full column rank,*

  then the solution to the closed-loop system asymptotically converges to the set

$$
\left\{ \left(I, V, \dot{I}, \dot{V}, u_s \right) : \dot{V} = 0, \dot{I} = 0, \dot{u}_s = 0, B^\top \left(I - \bar{I} \right) = 0 \right\}.
\tag{29}
$$

Proof. We use the integrated output port-variable to shape the desired closed-loop storage function, i.e.,

$$
S_d = S + \frac{1}{2} \left|\left| B^\top (I - \bar{I}) \right|\right|_{k_i}^2 ,
\tag{30}
$$

where S is given by (19). Then, S_d along the trajectories of system (20) controlled by (28) satisfies

$$
\dot{S}_d = -\dot{I}^\top R \dot{I} - \dot{V}^\top G \dot{V} + y_s^\top \left(v_s + k_i B^\top (I - \bar{I}) \right) \tag{31a}
$$
$$
= -\dot{I}^\top R \dot{I} - \dot{V}^\top G \dot{V} - k_d y_s^\top y_s + \mu_s^\top y_s \tag{31b}
$$
$$
\le \mu_s^\top y_s, \tag{31c}
$$

where in (31a) we use the controller (28). This concludes the proof of part (a). For part (b-i), let μ_s be equal to zero. Then, from (31b), there exists a forward invariant set Π and by LaSalle's invariance principle the solutions that start in Π converge to the largest invariant set contained in

$$
\Pi \cap \left\{ \left(I, V, \dot{I}, \dot{V}, u_s \right) : \dot{I} = 0, \dot{V} = 0 \right\}.
\tag{32}
$$

From (20c) it follows that $B v_s = 0$, i.e., $v_s = 0$ (B has full column rank). Moreover, from (28) it follows that $B^\top (I - \bar{I}) = 0$, concluding the proof of part (b-i). For part (b-ii), the solutions that start in the forward invariant set Π converge to the largest invariant set contained in

$$
\Pi \cap \left\{ \left(I, V, \dot{I}, \dot{V}, u_s \right) : R\dot{I} = 0, \dot{V} = 0, y_s = 0 \right\}.
\tag{33}
$$

On this invariant set, from (20d) we obtain $\Gamma^\top \dot{I} = 0$, which implies $\dot{I} = 0$ ($\Gamma^\top$ has full column rank). This further implies that, also in this case, the solutions starting in Π converge to the set (32). The rest of the proof follows from the proof of part (b-i). $\square$

Remark 8 (Alternative controller to (28))**.** *The controller (28) needs the information of the first time derivative of the inductor current. This can be avoided by rewriting (28) as follows:*

$$
\begin{aligned}
u_s &= -\left(k_i \phi + k_d B^\top I \right) \\
\dot{\phi} &= -\frac{1}{k_i} \mu_s + B^\top \left(I - \bar{I} \right).
\end{aligned}
\tag{34}
$$

By using the storage function (30), the same results of Theorem 1 can be established analogously. Moreover, note that (28) can be rewritten as in (34) because of the integrability of the port-variables.

We now extend this methodology to s–RLC circuits (11). One possible issue in extending this methodology to s–RLC circuits may be the integrability of the output port-variable y given by (25). In order to avoid this issue, we introduce the following assumption:

Assumption 7 (Integrating factor)**.** *There exist $m : \mathbb{R}^\sigma \times \mathbb{R}^\rho \to \mathbb{R}$ different from zero and $\gamma : \mathbb{R}^\sigma \times \mathbb{R}^\rho \to \mathbb{R}$ such that $\dot{\gamma} = my$.*

It is however worth to mention that the second methodology (i.e., *input shaping*) that we propose in Section III-C does not need Assumption 7. Relying on Assumption 7, the following lemma provides a new passive map with integrable output port-variable for system (24).

Lemma 1 (Integrable output)**.** *Let Assumptions 1, 2 and 7 hold. System (24) is passive with port-variables $\frac{v}{m}$ and $\dot{\gamma} = my$.*

Proof. After multiplying and dividing the last line of (26) by m, we obtain

$$
\dot{S} \le vy = \frac{v}{m} \dot{\gamma}.
$$

□

Theorem 2 (Output shaping for s–RLC circuits). *Let Assumptions 1–3 and 5–7 hold. Consider system (24) with control input υ given by*

$$\upsilon = m\left(\mu - k_i\left(\gamma - \gamma^\star\right) - k_d\dot\gamma\right), \qquad (35)$$

with $\gamma^\star = \gamma(\overline{I}, V^\star)$, $k_d > 0, k_i > 0$ and $\mu \in \mathbb{R}$. The following statements hold:

(a) *System (24) in closed-loop with control (35) defines a passive map $\mu \mapsto \dot\gamma$.*

(b) *Let μ be equal to zero. If any of the following conditions holds*
   (i) *$R > 0$ and $G > 0$*
   (ii) *$G > 0$, $\Gamma^\top(u)$ has full column rank, and*

$$\left(\Gamma_1 - \Gamma_0\right)V - \left(B_1 - B_0\right)V_s \neq 0, \qquad (36)$$

then the solution to the closed-loop system asymptotically converges to the set

$$\left\{\left(I, V, \dot I, \dot V, u\right) \mid \dot V = 0, \dot I = 0, \dot u = 0, \gamma = \gamma^\star\right\}. \quad (37)$$

Proof. We use the integrated output port-variable γ (see Lemma 1) to shape the desired closed-loop storage function, i.e.,

$$S_d = S + \frac{1}{2}k_i\left(\gamma - \gamma^\star\right)^2, \qquad (38)$$

where S is given by (19). Then, S_d along the trajectories of system (24) controlled by (35) satisfies

$$\dot S_d = -\dot I^\top R\dot I - \dot V^\top G\dot V + \frac{\upsilon}{m}\dot\gamma + k_i\left(\gamma - \gamma^\star\right)\dot\gamma \qquad (39a)$$

$$= -\dot I^\top R\dot I - \dot V^\top G\dot V - k_d\dot\gamma^2 + \mu\dot\gamma \qquad (39b)$$

$$\leq \mu\dot\gamma, \qquad (39c)$$

where in (39a) we use Proposition 2, Lemma 1 and the controller (35). This concludes the proof of part (a). For part (b-i), let μ be equal to zero. Then, from (39b), there exists a forward invariant set Π and by LaSalle's invariance principle the solutions that start in Π converge to the largest invariant set contained in

$$\Pi \cap \left\{\left(I, V, \dot I, \dot V, u_s\right) : \dot I = 0, \dot V = 0, \dot\gamma = 0\right\}. \quad (40)$$

On this invariant set, from (24c) and (24d) it follows that

$$\begin{bmatrix} \left(\Gamma_1 - \Gamma_0\right)V - \left(B_1 - B_0\right)V_s \\ \left(\Gamma_1 - \Gamma_0\right)^\top I \end{bmatrix} \upsilon = 0.$$

Then, according to Assumption 6, we have $\upsilon = 0$, which implies $\dot u = 0$. Moreover, from (35) it follows that $\gamma = \gamma^\star$, concluding the proof of part (b-i). For part (b-ii), when only G is positive definite, the solutions that start in the forward invariant set Π converge to the largest invariant set contained in

$$\Pi \cap \left\{\left(I, V, \dot I, \dot V, u_s\right) : R\dot I = 0, \dot V = 0, \dot\gamma = 0\right\}. \quad (41)$$

On this invariant set, from (24c) and (36) we obtain $\upsilon = 0$. Consequently, from (24d) we have $\Gamma^\top(u)\dot I = 0$, which implies $\dot I = 0$ ($\Gamma^\top(u)$ has full column rank). This further implies that, also in this case, the solutions starting in Π converge to the

set (40). The rest of the proof follows from the proof of part (b-i). □

Remark 9 (Output shaping stability). *Theorems 1 and 2 imply that the integrated output port-variables converge to the corresponding desired values and the first time derivatives of the state converge to zero. However, this generally does not imply that the trajectories of the closed-loop system asymptotically converge to the corresponding desired operating point[§§]. Furthermore, for the buck, boost, buck-boost and Cúk applications (see Section IV and Appendix), we will show that Theorems 1 and 2 also imply that all the trajectories of the closed-loop system asymptotically converge to the corresponding desired operating point. We also notice that for the input shaping methodology that we present in next subsection, under some mild and reasonable assumptions, the stability results will be strengthened.*

Remark 10 (Limitations of output shaping). *Note that, if the resistance R of a RLC circuit is negligible, then, in order to establish the stability results presented in Theorem 2 part (b-ii), condition (36) needs to be satisfied. More specifically, for a buck converter (see Section IV-A), this is equivalent to have $V_s \neq 0$, which is in practice true (see also Assumption 3). Yet, for a boost converter (see Section IV-B), satisfying condition (36) is equivalent to require $V \neq 0$, which generally could be not always true. Moreover, the output shaping control methodology relies on finding γ satisfying $\dot\gamma = my$, with $m \neq 0$. This may not always be possible. Finally, designing a controller based on the output shaping methodology requires the information of $\overline{I}$, which often depends on the load parameters. Consequently, the output shaping methodology is sensitive to load uncertainty (see Remark 5).*

C. Input Shaping

The second methodology, which we call *input shaping*, relies on the integrability property of the *input* port-variables υ_s and υ (see Proposition 1 and Proposition 2), respectively. Similarly to the output shaping technique, we use the integrated input port-variable to shape the closed-loop storage function such that it has a minimum at the desired operating point (see Objective 1). Compared to the output shaping methodology, the input shaping methodology has the following advantages:

(i) Assumption 7 on the integrability of the output port-variable is no longer needed;
(ii) the knowledge of $\bar u_s$ and $\bar u$, given by (16) and (17), respectively, does not usually require the information of the load parameters (see the examples in Subsections IV-A and IV-B), making the input shaping control methodology robust with respect to load uncertainty;
(iii) condition (36) is not required anymore and, in addition, all the trajectories of the extended system converge to the desired operating point.

[§§]If $\sigma = m$, the input matrix becomes a full rank matrix and, as a consequence, in case of RLC circuits, asymptotic convergence to the corresponding desired operating point can be proved.

We now first present the input shaping methodology for RLC circuits (3).

Theorem 3 (Input shaping for RLC circuits). *Let Assumptions 1–4 hold. Consider system* (20) *with control input υ_s given by*

$$\upsilon_s = \frac{1}{k_d}\left(\mu_s - k_i\left(u_s - \bar{u}_s\right) - y_s\right), \qquad (42)$$

with $y_s = B^\top \dot{I}$, $k_d > 0$, $k_i > 0$ and $\mu_s \in \mathbb{R}^m$. The following statements hold:

(a) *System* (20) *in closed-loop with control* (42) *defines a passive map $\mu_s \mapsto \dot{u}_s$ (note that u_s is a state of the extended system* (20)).

(b) *Let μ_s be equal to zero. If any of the following conditions holds*

   (i) $R > 0$ *and* $G > 0$
   (ii) $R > 0$ *and* Γ *has full column rank*
   (iii) $G > 0$ *and* $\Gamma^\top$ *has full column rank,*

   then the solution to the closed-loop system asymptotically converges to the set

$$\left\{\left(I, V, \dot{I}, \dot{V}, u_s\right) : \dot{V} = 0, \dot{I} = 0, \dot{u}_s = 0, u_s = \bar{u}_s\right\}. \qquad (43)$$

(c) *If any of the conditions in (b) holds and the matrix*

$$\mathcal{A}_s = \begin{bmatrix} R & \Gamma \\ \Gamma^\top & -G \end{bmatrix} \qquad (44)$$

   has full-rank, then the solution to the closed-loop system asymptotically converges to the desired operating point $\left(\bar{I}, V^\star, 0, 0, \bar{u}_s\right)$, which is unique.

Proof. We use the integrated input port-variable to shape the desired closed-loop storage function, i.e,

$$S_d = S + \frac{1}{2}\left\|u_s - \bar{u}_s\right\|_{k_i}^2, \qquad (45)$$

where S is given by (19). Then, S_d along the trajectories of system (20) controlled by (42) satisfies

$$\dot{S}_d = -\dot{I}^\top R\dot{I} - \dot{V}^\top G\dot{V} + \dot{u}_s^\top\left(y_s + k_i\left(u_s - \bar{u}_s\right)\right) \quad (46a)$$

$$= -\dot{I}^\top R\dot{I} - \dot{V}^\top G\dot{V} - k_d\dot{u}_s^\top\dot{u}_s + \mu_s^\top\dot{u}_s \quad (46b)$$

$$\leq \mu_s^\top\dot{u}_s, \qquad (46c)$$

where in (46a) we use Proposition 1 and the controller (42). This concludes the proof of part (a). For part (b-i), let μ_s be equal to zero. Then, from (46b), there exists a forward invariant set Π and by LaSalle's invariance principle the solutions that start in Π converge to the largest invariant set contained in

$$\Pi \cap \left\{\left(I, V, \dot{I}, \dot{V}, u_s\right) : \dot{I} = 0, \dot{V} = 0, \dot{u}_s = 0\right\}. \qquad (47)$$

On this invariant set, $\dot{I} = 0$ and $\dot{u}_s = 0$ further imply $y_s = 0$ and $\upsilon_s = 0$, respectively. Consequently, from (42) it follows that $u_s = \bar{u}_s$, concluding the proof of part (b-i). For part (b-ii) and (b-iii), the solutions that start in the forward invariant set Π converge to the largest invariant set contained in

$$\Pi \cap \left\{\left(I, V, \dot{I}, \dot{V}, u_s\right) : R\dot{I} = 0, G\dot{V} = 0, \dot{u}_s = 0\right\}. \qquad (48)$$

On this set, from (20c) and (20d) we get $\Gamma\dot{V} = 0$ and $\Gamma^\top\dot{I} = 0$, respectively. Consequently, if (b-ii) or (b-iii) holds, then $\dot{I} = 0$ and $\dot{V} = 0$. This further implies that the solutions that start in Π converge to the set (47). The rest of the proof follows from the proof of part (b). For part (c), we first notice that from (16) we have

$$\begin{bmatrix} \bar{I} \\ V^\star \end{bmatrix} = \mathcal{A}_s^{-1}\begin{bmatrix} B\bar{u}_s \\ 0 \end{bmatrix}, \qquad (49)$$

implying that $\left(\bar{I}, V^\star\right)$ is unique. Moreover, on the set (47), from (20a) and (20b) we obtain

$$\begin{bmatrix} I \\ V \end{bmatrix} = \mathcal{A}_s^{-1}\begin{bmatrix} B\bar{u}_s \\ 0 \end{bmatrix}. \qquad (50)$$

Then, from (49), I and V converge to $\bar{I}$ and $V^\star$, respectively. $\square$

We now extend these results to s–RLC circuits (11).

Theorem 4 (Input shaping for s–RLC circuits). *Let Assumptions 1–3, 5 and 6 hold. Consider system* (24) *with control input υ given by*

$$\upsilon = \frac{1}{k_d}\left(\mu - k_i\left(u - \bar{u}\right) - y\right), \qquad (51)$$

with y given by (25), *$k_d > 0, k_i > 0$ and $\mu \in \mathbb{R}$. The following statements hold:*

(a) *System* (24) *in closed-loop with control* (51) *defines a passive map $\mu \mapsto \dot{u}$ (note that u is a state of the extended system* (24)).

(b) *Let μ be equal to zero. If any of the following conditions holds*

   (i) $R > 0$ *and* $G > 0$
   (ii) $R > 0$ *and* $\Gamma(u)$ *has full column rank*
   (iii) $G > 0$ *and* $\Gamma^\top(u)$ *has full column rank,*

   then the solution to the closed-loop system asymptotically converges to the set

$$\left\{\left(I, V, \dot{I}, \dot{V}, u\right) \mid \dot{V} = 0, \dot{I} = 0, \dot{u} = 0, u = \bar{u}\right\}. \qquad (52)$$

(c) *If any of the conditions in (b) holds and the matrix*

$$\mathcal{A} = \begin{bmatrix} R & \Gamma(\bar{u}) \\ \Gamma^\top(\bar{u}) & -G \end{bmatrix} \qquad (53)$$

   has full-rank, then the solution to the closed-loop system asymptotically converges to the desired operating point $\left(\bar{I}, V^\star, 0, 0, \bar{u}\right)$, which is unique.

Proof. We use the integrated input port-variable to shape the desired closed-loop storage function, i.e.,

$$S_d = S + \frac{1}{2}k_i\left(u - \bar{u}\right)^2, \qquad (54)$$

where S is given by (19). Then, by using the storage function (54), the proof is analogous to that of Theorem 3. $\square$

Remark 11 (Robustness property of input shaping methodology). *Note that the controllers* (42) *and* (51) *proposed in Theorems 3 and 4, respectively, require information of the desired value of the control input. If $R = 0$, from the first line of* (16) *and* (17), *it follows that $\bar{u}_s$ and $\bar{u}$ require only*
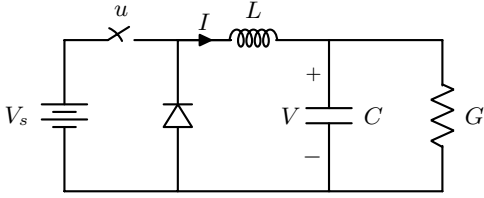
Figure 1. Electrical scheme of the buck converter.

information of the desired voltage $V^\star$. This implies that the input shaping methodology is robust with respect to load uncertainty (see Remark 5).

Remark 12 (Initial conditions for u_s and u)**.** *The control inputs u and u_s of systems* (3) *and* (8) *are states of the extended systems* (20) *and* (24)*, respectively. Moreover, we proved that the closed-loop dynamics of these extended systems are asymptotically stable. Therefore, independently of the initial conditions of u and u_s, the proposed dynamic controllers stabilize the corresponding closed-loop systems to their desired operating points.*

Before showing the application of the proposed control methodologies to power converters in the next section, we notice that, under certain assumptions on Γ, the input shaping methodology allows for $R \geq 0$ or $G \geq 0$. Differently, the output shaping methodology allows only for $R \geq 0$. Furthermore, under certain assumptions on the steady state equations, the input shaping methodology guarantees that *all* the solutions to the extended system converge to the desired operating point.

IV. APPLICATION TO DC-DC POWER CONVERTERS

In this section, we use the control methodologies proposed in the previous section for regulating the output voltage of the most widespread DC-DC power converters: the buck and the boost converters[¶¶], respectively.

A. Buck converter

Consider the electrical scheme of the buck converter in Figure 1, where the diode is assumed to be ideal. Then, by applying the Kirchhoff's current (KCL) and voltage (KVL) laws, the *average* governing dynamic equations of the buck converter are the following:

$$-L\dot{I} = V - uV_s$$
$$C\dot{V} = I - GV. \tag{55}$$

Equivalently, system (55) can be obtained from (11) with $\Gamma_0 = \Gamma_1 = 1$, $B_0 = 0$, $B_1 = 1$ and $R = 0$. By using Proposition 2, the following passivity property is established.

[¶¶]Buck and boost converters describe in form and function a large family of DC-DC power converters. Moreover, in Appendices A and B we also study other two common types of DC-DC power converters: the buck-boost and Cúk converters

Lemma 2 (Passivity property of the buck converter)**.** *Let Assumptions 1 and 2 hold. System* (55) *is passive with respect to the storage function* (19) *and the port-variables $\dot{u}$ and $\dot{I}V_s$.*

By virtue of the above passivity property, we can now use the output shaping and input shaping control methodologies to design voltage controllers.

Corollary 1 (Output shaping for the buck converter)**.** *Let Assumptions 1–3 and 5 hold. Consider system* (55) *with the dynamic controller*

$$\dot{u} = -V_s \left(k_i \left(I - \overline{I} \right) + k_d \dot{I} \right), \tag{56}$$

with $k_d > 0$ and $k_i > 0$. Then, the solution (I, V, u) to the closed-loop system asymptotically converges to the desired steady-state $\left(\overline{I}, V^\star, \overline{u} \right)$.

Proof. For the buck converter (55), condition (36) is equivalent to require $V_s \neq 0$, which holds by Assumption 3. Consequently, Theorem 2 can be used by selecting $m = 1$, $\gamma = IV_s$ and $\gamma^\star = \overline{I}V_s$. In analogy with Theorem 2, the solutions to the closed-loop system converge to the set

$$\Pi \cap \left\{ (I, V, u) : \dot{I} = 0, \dot{V} = 0 \right\}. \tag{57}$$

By differentiating the first line of (55), on this invariant set we get $\dot{u} = 0$. As a consequence, from (56) it follows that $I = \overline{I}$ which further implies $V = V^\star$ and $u = \overline{u}$ (see Assumption 5). $\square$

Corollary 2 (Input shaping for the buck converter)**.** *Let Assumptions 1–3 and 5 hold. Consider system* (55) *with the dynamic controller*

$$\dot{u} = -\frac{1}{k_d} \left(k_i \left(u - \overline{u} \right) + V_s \dot{I} \right), \tag{58}$$

with $k_d > 0$ and $k_i > 0$. Then, the solution (I, V, u) to the closed-loop system asymptotically converges to the desired steady-state $\left(\overline{I}, V^\star, \overline{u} \right)$.

Proof. The proof is analogous to that of Theorem 4. $\square$

B. Boost converter

Consider now the electrical scheme of the boost converter in Figure 2, where the diode is again assumed to be ideal. The *average* governing dynamic equations of the boost converter are the following:

$$-L\dot{I} = (1 - u)V - V_s$$
$$C\dot{V} = (1 - u)I - GV. \tag{59}$$

Also in this case, system (59) can be obtained from (11) with $\Gamma_0 = 1$, $\Gamma_1 = 0$, $B_0 = B_1 = 1$ and $R = 0$. By using Proposition 2, the following passivity property is established.

Lemma 3 (Passivity property of boost converter)**.** *Let Assumptions 1 and 2 hold. System* (59) *is passive with respect to the storage function* (19) *and the port-variables $\dot{u}$ and $\dot{I}V - \dot{V}I$.*

Remark 13 (Integrable output port-variables for the boost converter)**.** *Note that the output port-variable $\dot{I}V - \dot{V}I$ is not integrable. It is however possible to find a different*
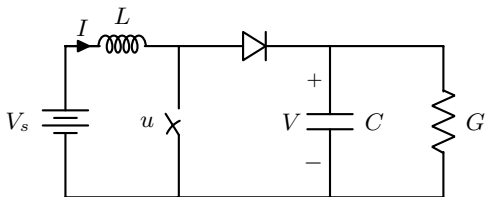
Figure 2. Electrical scheme of the boost converter.

Table II
PASSIVE MAPS FOR THE BOOST-CONVERTER

$m(I,V)$	Passive map	$\gamma(I,V)$
1	$\dot{u} \mapsto \dot{I}V - \dot{V}I$	
$\dfrac{1}{V^2}$	$V^2\dot{u} \mapsto \dfrac{d}{dt}\dfrac{I}{V}$	$\dfrac{I}{V}$
$\dfrac{1}{I^2}$	$I^2\dot{u} \mapsto -\dfrac{d}{dt}\dfrac{V}{I}$	$-\dfrac{V}{I}$
$\dfrac{1}{V^2+I^2}$	$(V^2+I^2)\dot{u} \mapsto \dfrac{d}{dt}\tan^{-1}\left(\dfrac{I}{V}\right)$	$\tan^{-1}\left(\dfrac{I}{V}\right)$
$\dfrac{1}{IV}$	$(IV)\dot{u} \mapsto \dfrac{d}{dt}ln\left(\dfrac{I}{V}\right)$	$ln\left(\dfrac{I}{V}\right)$

output port-variable that is indeed integrable (see Lemma 1). More precisely, if we choose for instance $m = 1/I^2$, we obtain the passive map $\dot{u}I^2 \mapsto -\frac{d}{dt}(V/I)$ (see Table II for different passivity properties corresponding to different choices of (integrable) output port-variables).

By virtue of the above passivity property, we can now use the output shaping and input shaping control methodologies to design voltage controllers.

Corollary 3 (Output shaping for the boost converter)**.** *Let Assumptions 1–3 and 5 hold. Moreover, let $V(t)$ be different from zero for any $t \geq 0$. Consider system (55) with the dynamic controller*

$$\dot{u} = -\frac{1}{V^2}\left(k_i\left(\frac{I}{V} - \frac{\bar{I}}{V^\star}\right) + k_d\frac{d}{dt}\frac{I}{V}\right), \qquad (60)$$

with $k_d > 0$ and $k_i > 0$. Then, the solution (I,V,u) to the closed-loop system asymptotically converges to the desired steady-state $\left(\bar{I}, V^\star, \bar{u}\right)$.

Proof. For the boost converter (59), condition (36) is equivalent to require $V(t) \neq 0$ for any $t \geq 0$, which holds by assumption. Consequently, Theorem 2 can be used by selecting for instance $m = 1/V^2$, $\gamma = I/V$ and $\gamma^\star = \bar{I}/V^\star$. In analogy with Theorem 2, the solutions to the closed-loop system converge to the set

$$\Pi \cap \left\{(I,V,u) : \dot{V} = 0, \dot{I} = 0\right\}. \qquad (61)$$

By differentiating the first line of (59), on this invariant set we get $\dot{u} = 0$. As a consequence, from (60) it follows that $\gamma = \gamma^\star$. Then, from the second line of (59) it yields

$$u = 1 - G\frac{V}{I} = 1 - G\frac{1}{\gamma} = 1 - G\frac{V^\star}{\bar{I}} = \bar{u}, \qquad (62)$$

which further implies $V = V^\star$ and $I = \bar{I}$. $\qquad\square$

Corollary 4 (Input shaping for boost converter)**.** *Let Assumptions 1–3, 5 and 6 hold[***]. Consider system (59) with the dynamic controller*

$$\dot{u} := -\frac{1}{k_d}\left(k_i\left(u - \bar{u}\right) + \left(\dot{I}V - \dot{V}I\right)\right), \qquad (63)$$

with $k_d > 0$ and $k_i > 0$. Then, the solution (I,V,u) to the closed-loop system asymptotically converges to the desired steady-state $\left(\bar{I}, V^\star, \bar{u}\right)$.

Proof. The proof is analogous to that of Theorem 4. $\qquad\square$

In Table IV we have summerized the passivity properties derived in the pH [2], BM [25] and proposed framework, respectively.

For the sake of completeness, we now show in Figures 3–6 the simulation results obtained by implementing the proposed methodologies to control the output voltage of a buck and boost converter, respectively. In order to verify the robustness property of the proposed controllers with respect to the load uncertainty, the value of the load is changed from G to $G + \Delta G$, with ΔG uncertain, at the time instant $t = 1\,\text{s}$ (all the simulation parameters are reported at the end of the caption of each figure). More precisely, Figures 3 and 5 show that after the load variation the voltage converges to a steady state value different from the desired one. Controllers (56) and (60) depend indeed on $\bar{I} = GV^\star$ and, therefore, require the information of G. On the contrary, Figures 4 and 6 clearly show that the input shaping methodology is robust with respect to load uncertainty (see also Remark 11). Furthermore, for the sake of fairness, we compare the proposed input shaping methodology with the *Parallel Damping PBC* approach proposed in [20, Section V]. Figures 3 and 5 indicate that *Parallel Damping PBC* approach is also robust with respect to load variation. However, it is important to note that the *Parallel Damping PBC* approach requires the information of the filter inductance L and capacitance C.

C. DC Networks

In this subsection we consider a typical DC microgrid of which a schematic electrical diagram is provided in Figure 7, including a buck and boost DC-DC power converter interconnected through resistive-inductive power lines. In the following we adopt the subscripts α or β in order to refer to the buck or boost type converter, respectively. The network consists of n_α buck converters and n_β boost converters, such that the total number of converters is $n_\alpha + n_\beta = n$. The overall network is represented by a connected and undirected graph $\mathcal{G} = (\mathcal{V}_\alpha \cup \mathcal{V}_\beta, \mathcal{E})$, where $\mathcal{V}_\alpha = \{1, \ldots, n_\alpha\}$ is the set of the buck converters, $\mathcal{V}_\beta = \{n_\alpha + 1, \ldots, n\}$ is the set of the boost converters and $\mathcal{E} = \{1, ..., m\}$ is the set of the distribution lines interconnecting the n converters. The network topology is

---

[***]For the boost converter, Assumption 6 is equivalent to require that V and I are not equal to zero at the same time (i.e., V can be equal to zero when I is different from zero and vice versa). We note that to use the output shaping methodology we need a stronger assumption, i.e., V different from zero for any $t \geq 0$ (see Corollary 3).
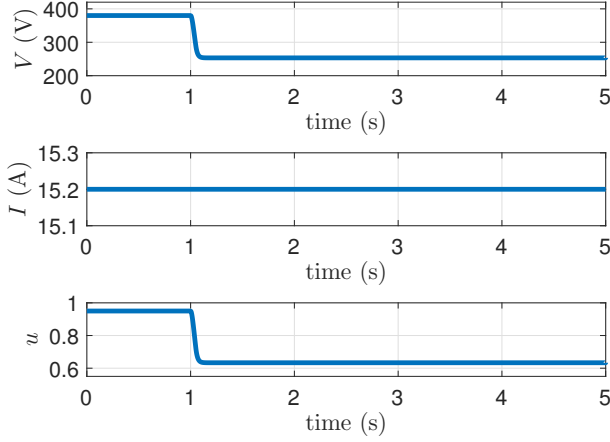
Figure 3. (Output shaping for the buck converter) From the top: time evolution of the voltage, current and duty cycle considering a load variation ΔG at the time instant $t = 1$ s (Parameters: $L = 1$ mH, $C = 1$ mF, $V_s = 400$ V, $G = 0.04$ S, $\Delta G = 0.02$ S, $V^\star = 380$ V, $k_d = 5 \times 10^5$, $k_i = 1 \times 10^7$).

Figure 5. (Output shaping for the boost converter) From the top: time evolution of the voltage, current and duty cycle considering a load variation at the time instant $t = 1$ s (Parameters: $L = 1.12$ mH, $C = 6.8$ mF, $V_s = 280$ V, $G = 0.04$ S, $\Delta G = -0.02$ S, $V^\star = 380$ V, $k_d = 5 \times 10^2$, $k_i = 1 \times 10^6$).

Figure 4. (Input shaping for the buck converter) From the top: time evolution of the voltage, current and duty cycle considering a load variation ΔG at the time instant $t = 1$ s. Input shaping for buck converter is plotted in blue color, while *Parallel Damping PBC* approach proposed in [20] is plotted in red-dashed. (Parameters: $L = 1$ mH, $C = 1$ mF, $V_s = 400$ V, $G = 0.04$ S, $\Delta G = 0.02$ S, $V^\star = 380$ V, $k_d = 16 \times 10^5$, $k_i = 8 \times 10^7$, $\bar{u} = V^\star/V_s$ and gamma in [20, Equation (19)] is set to 0.97).
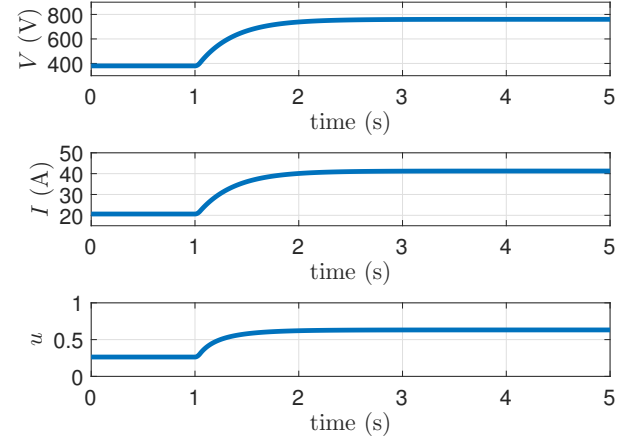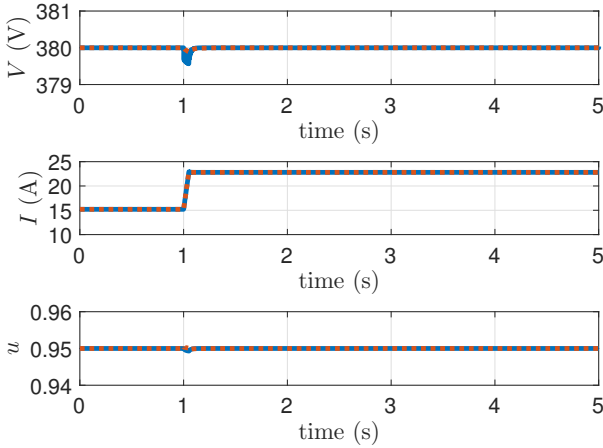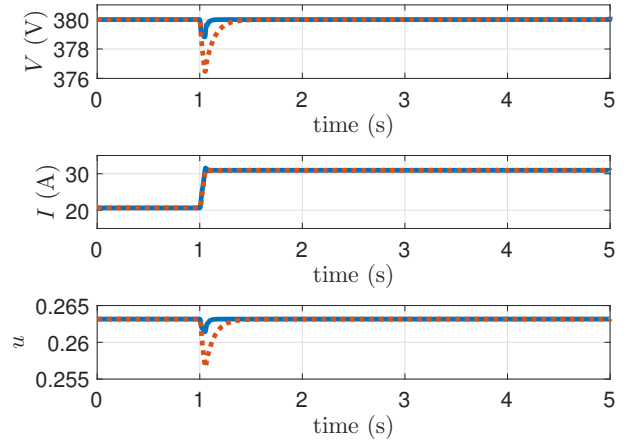
Figure 6. (Input shaping for the boost converter) From the top: time evolution of the voltage, current and duty cycle considering a load variation at the time instant $t = 1$ s. Input shaping for boost converter is plotted in blue color, while *Parallel Damping PBC* approach proposed in [20] is plotted in red-dashed. (Parameters: $L = 1.12$ mH, $C = 6.8$ mF, $V_s = 280$ V, $G = 0.04$ S, $\Delta G = 0.02$ S, $V^\star = 380$ V, $k_d = 1 \times 10^6$, $k_i = 4 \times 10^7$, $\bar{u} = 1 - V_s/V^\star$ and gamma in [20, Equation (23)] is set to 0.1.)

represented by its corresponding incidence matrix $\mathrm{D} \in \mathbb{R}^{n \times m}$. The ends of edge k are arbitrarily labeled with a $+$ and a $-$, and the entries of D are given by

$$\mathrm{D}_{ik} = \begin{cases} +1 & \text{if } i \text{ is the positive end of } k \\ -1 & \text{if } i \text{ is the negative end of } k \\ 0 & \text{otherwise.} \end{cases}$$

According to (55), the average dynamic equations of the buck converter $i \in \mathcal{V}_\alpha$ become

$$-L_i \dot{I}_i = V_i - u_i V_{si}$$
$$C_i \dot{V}_i = I_i - G_i V_i - \sum_{k \in \mathcal{E}_i} I_{lk}, \tag{64}$$

where $\mathcal{E}_i \subset \mathcal{E}$ is the set of the distribution lines incident to the node i, and I_{lk} denotes the current through the line $k \in \mathcal{E}_i$. On the other hand, according to (59), the average dynamic

Figure 7. The considered electrical diagram of a (Kron reduced) DC network representing node $i \in \mathcal{V}_\alpha$ and node $j \in \mathcal{V}_\beta$ interconnected by the line $k \in \mathcal{E}$.

equations of the boost converter $i \in \mathcal{V}_\beta$ become
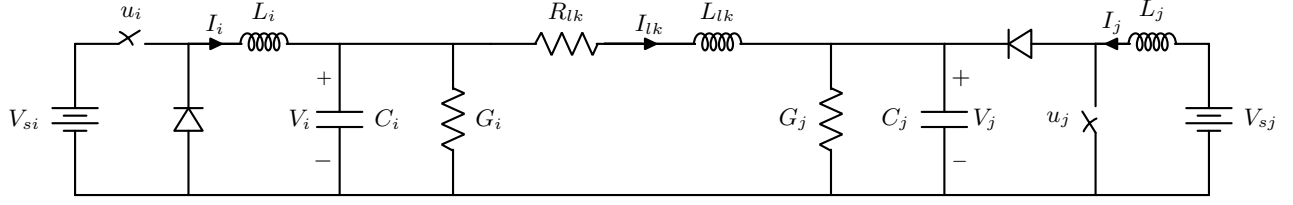
$$-L_i \dot{I}_i = (1 - u_i)V_i - V_{si}$$
$$C_i \dot{V}_i = (1 - u_i)I_i - G_i V_i - \sum_{k \in \mathcal{E}_i} I_{lk}. \tag{65}$$

The dynamic of the current I_{lk} from node i to node $j \neq i$, $i, j \in \mathcal{V}_\alpha \cup \mathcal{V}_\beta$, is given by

$$-L_{lk}\dot{I}_{lk} = -(V_i - V_j) + R_{lk}I_{lk}. \tag{66}$$

Let $V = [V_\alpha^\top, V_\beta^\top]^\top$, with $V_\alpha = [V_1, \ldots, V_{n_\alpha}]$ and $V_\beta = [V_{n_\alpha+1}, \ldots, V_n]$. Analogously, let $I_\alpha = [I_1, \ldots, I_{n_\alpha}]$ and $I_\beta = [I_{n_\alpha+1}, \ldots, I_n]$. To study the interconnected DC network, we write (64)-(66) compactly for all buses $i \in \mathcal{V}_\alpha \cup \mathcal{V}_\beta$

$$-L_\alpha \dot{I}_\alpha = V_\alpha - u_\alpha \circ V_{s\alpha} \tag{67a}$$
$$-L_\beta \dot{I}_\beta = (\mathbb{1}_{n_\beta} - u_\beta) \circ V_\beta - V_{s\beta} \tag{67b}$$
$$-L_l \dot{I}_l = \mathrm{D}^T V + R_l I_l \tag{67c}$$
$$C_\alpha \dot{V}_\alpha = I_\alpha - G_\alpha V_\alpha + \mathrm{D}_\alpha I_l \tag{67d}$$
$$C_\beta \dot{V}_\beta = (\mathbb{1}_{n_\beta} - u_\beta) \circ I_\beta - G_\beta V_\beta + \mathrm{D}_\beta I_l, \tag{67e}$$

where $I_\alpha, V_\alpha, V_{s\alpha}, u_\alpha \in \mathbb{R}^{n_\alpha}$, $I_\beta, V_\beta, V_{s\beta}, u_\beta \in \mathbb{R}^{n_\beta}$, $I_l \in \mathbb{R}^m$. Moreover, $L_\alpha, L_\beta, L_l, C_\alpha, C_\beta, R_l, G_\alpha, G_\beta$, are positive definite diagonal matrices of appropriate dimensions, e.g. $L_\alpha = \mathrm{diag}(L_1, \ldots, L_{n_\alpha})$, and $\mathbb{1}_{n_\beta} \in \mathbb{R}^{n_\beta}$ denotes the vector consisting of all ones. The matrices $\mathrm{D}_\alpha \in \mathbb{R}^{n_\alpha \times m}$ and $\mathrm{D}_\beta \in \mathbb{R}^{n_\beta \times m}$ are obtained by collecting from D the rows indexed by $\mathcal{V}_\alpha$ and $\mathcal{V}_\beta$, respectively. Let $I = [I_\alpha^\top, I_\beta^\top, I_l^\top]^\top$, $u = [u_\alpha^\top, u_\beta^\top]^\top$, $V_s = [V_{s\alpha}^\top, V_{s\beta}^\top]^\top$, $L = \mathrm{diag}(L_\alpha, L_\beta, L_l)$ and $C = \mathrm{diag}(C_\alpha, C_\beta)$. We notice that system (67) can be expressed in the BM formulation (8) with

$$B(u) = \begin{bmatrix} \mathrm{diag}(u_\alpha) & \mathbf{0}^{n_\alpha \times n_\beta} \\ \mathbf{0}^{n_\beta \times n_\alpha} & \mathbb{I}_{n_\beta} \\ \mathbf{0}^{m \times n_\alpha} & \mathbf{0}^{m \times n_\beta} \end{bmatrix}, \tag{68}$$

and

$$P(u, I, V) = I^\top \Gamma(u) V + \frac{1}{2} I_l^\top R_l I_l \\ - \frac{1}{2} V_\alpha^\top G_\alpha V_\alpha - \frac{1}{2} V_\beta^\top G_\beta V_\beta, \tag{69}$$

where $\Gamma \in \mathbb{R}^{(n+m) \times n}$ is given by

$$\Gamma(u) = \begin{bmatrix} \mathbb{I}_{n_\alpha} & \mathbf{0}^{n_\alpha \times n_\beta} \\ \mathbf{0}^{n_\beta \times n_\alpha} & \mathbb{I}_{n_\beta} - \mathrm{diag}(u_\beta) \\ \mathrm{D}_\alpha^T & \mathrm{D}_\beta^T \end{bmatrix}, \tag{70}$$

$\mathbb{I}$ being the identity matrix. By using now the storage function in (19), the following passivity property for the considered DC network (67) is established.

Lemma 4 (Passivity property of DC Networks). *Let Assumptions 1 and 2 hold. System (67) is passive with respect to the storage function (19) and the port-variables $\dot{u}$ and*

$$y_{\mathrm{DC}} = \begin{bmatrix} \dot{I}_\alpha \circ V_{s\alpha} \\ \dot{I}_\beta \circ V_\beta - \dot{V}_\beta \circ I_\beta \end{bmatrix}. \tag{71}$$

By virtue of the above passivity property, we can now use the input shaping methodology to design a decentralized control scheme for regulating the voltage of (67).

Proposition 3 (Input shaping for DC Networks). *Let Assumptions 1–3, 5 and 6 hold. Consider system (67) with the dynamic controller*

$$\dot{u} = -K_d^{-1} \left(K_i (u - \bar{u}) + y_{\mathrm{DC}} \right), \tag{72}$$

where K_d and K_i are positive definite diagonal matrices of order $n_\alpha + n_\beta$, and y_{DC} is given by (71). Then, the solution (I, V, u) to the closed-loop system asymptotically converges to the desired steady-state $(\bar{I}, V^\star, \bar{u})$.

Proof. Consider the storage function (19). We use the integrated input port-variable to shape the desired closed-loop storage function, i.e.,

$$S_d = S + \frac{1}{2} (u - \bar{u})^\top K_i (u - \bar{u}). \tag{73}$$

Then, the first time derivative of S_d along the trajectories of system (67) controlled by (72) satisfies

$$\dot{S}_d = -\dot{I}_l^\top R_l \dot{I}_l - \dot{V}^\top G \dot{V} + \dot{u}^\top y_{DC} + \dot{u}^\top K_i (u - \bar{u}) \tag{74a}$$
$$= -\dot{I}_l^\top R_l \dot{I}_l - \dot{V}^\top G \dot{V} - \dot{u}^\top K_d \dot{u}, \tag{74b}$$

where we use Lemma 4 and the controller (72). Then, from (74b) there exists a forward invariant set Π and by LaSalle's invariance principle the solutions that start in Π converge to the largest invariant set contained in

$$\Pi \cap \left\{ \left(I, V, \dot{I}, \dot{V}, u \right) : \dot{I}_l = 0, \dot{V} = 0, \dot{u} = 0 \right\}. \tag{75}$$

On this invariant set, by differentiating (67d) and (67e) we get $\dot{I} = 0$. Moreover, from (72) it follows that $u = \bar{u}$, which further implies $V = V^\star$ and $I = \bar{I}$. $\square$

The proposed decentralized control scheme is now assessed in simulation[†††], considering a DC network comprising four

[†††]For the readers interested also in experimental results obtained by implementing the input shaping control methodology in a real DC microgrid comprising boost converters, we refer to [39].

Table III
NETWORK PARAMETERS

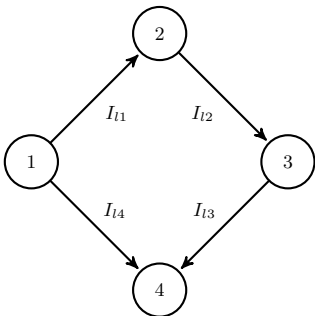| Node		1	2	3	4
L_i	(mH)	1.8	1.12	3.0	1.12
C_i	(mF)	2.2	6.8	2.5	6.8
V_{si}	(V)	400.0	280.0	450.0	320.0
$V_i^\star$	(V)	380.0	380.0	380.0	380.0
G	(S)	0.08	0.04	0.05	0.07
ΔG	(S)	0.01	0.03	-0.03	0.01

Figure 8. Scheme of the considered network with 4 power converters: Nodes 1 and 3 have buck converters, Nodes 2 and 4 have boost converters.

power converters (i.e., two buck and two boost converters) interconnected as shown in Figure 8. The parameters of the converters and lines are reported in Table III and [31, Table III], respectively. The controller gains for the buck converters are $k_{d\alpha} = 4 \times 10^5$ and $k_{i\alpha} = 4 \times 10^7$, while for the boost converters are $k_{d\beta} = 1 \times 10^6$ and $k_{i\beta} = 4 \times 10^7$. The most significant electrical signals of the simulation results are shown in Figure 9. In order to verify the robustness property of the control scheme with respect to the load uncertainty, the value of the load is changed from G to $G + \Delta G$ at the time instant $t = 1\,\mathrm{s}$ (see Table III). One can appreciate that the input shaping methodology is robust with respect to load uncertainty (see Remark 11).

V. CONCLUSIONS AND FUTURE WORKS

In this paper, we have presented new passivity properties for a class of RLC and s–RLC circuits that are modeled using the Brayton-Moser formulation. We use these new passivity properties to propose two new control methodologies: *output shaping* and *input shaping*. The key observations are:

(i) The output shaping methodology exploits the integrability property of the output port-variable. The input shaping technique instead exploits the integrability property of the input port-variable.

(ii) The controllers based on the input shaping methodology show robustness properties with respect to load uncertainty.

Possible future directions include to incorporate nonlinear loads (e.g. constant power loads [39], [40]), develop distributed control schemes (e.g. for achieving load sharing [41]) and extend such a new passivity concept to a wider class of nonlinear systems [42], [43].
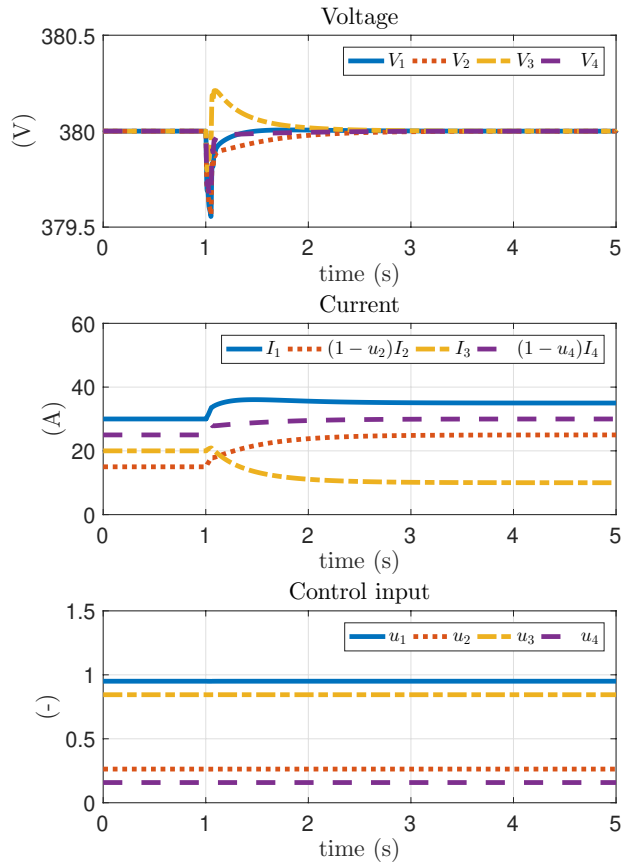
Figure 9. (Input shaping for the DC network) From the top: time evolution of the voltage of each node, current generated by each converter and duty cycle of each converter, considering a load variation at the time instant $t = 1$ s.

APPENDIX

In this Appendix we use the input shaping methodology to design voltage controllers for the buck-boost and Cúk converters, respectively. The proofs of the following Corollaries are analogous to those of Corollaries 2 and 4 presented in Section IV.

A. Buck-boost Converter

The average governing dynamic equations of the buck-boost converter are the following:

$$-L\dot{I} = (1 - u)V - uV_s$$
$$C\dot{V} = (1 - u)I - GV. \tag{76}$$

Equivalently, system (76) can be obtained from (11) with $\Gamma_0 = 1$, $\Gamma_1 = 0$, $B_0 = 0$, $B_1 = 1$ and $R = 0$. By using Proposition 2, the following passivity property is established.

Lemma 5 (Passivity property of the buck-boost converter)**.** *Let Assumptions 1 and 2 hold. System* (76) *is passive with respect to the storage function* (19) *and the port-variables $\dot{u}$ and $y = \dot{I}V - \dot{V}I + V_s\dot{I}$.*

TABLE IV
SUPPLY-RATES OF RLC AND s–RLC CIRCUITS

framework	supply-rate				
	RLC	s–RLC	buck	boost	buck-boost
Port–Hamiltonian	$I^\top B u_s$	$I^\top B(u)V_s = I^\top B_0 V_s + uI^\top\left(B_1 - B_0\right)V_s$	uIV_s	IV_s	uIV_s
Brayton–Moser	$\dot{I}^\top B u_s$	-	$uI\dot{V}_s$	-	-
Proposed	$\dot{I}^\top B \dot{u}_s$	$\dot{u}(\dot{V}^\top(\Gamma_1 - \Gamma_0)^\top I - \dot{I}^\top(\Gamma_1 - \Gamma_0)V - \dot{I}^\top(B_0 - B_1)V_s)$	$\dot{u}IV_s$	$\dot{u}\left(\dot{I}V - \dot{V}I\right)$	$\dot{u}\left(\dot{I}V - \dot{V}I + V_s\dot{I}\right)$

By virtue of the above passivity property, we can now use the input shaping methodology to design a voltage controller.

Corollary 5 (Input shaping for the buck-boost converter). *Let Assumptions 1–3, 5 and 6 hold. Consider system (76) with the dynamic controller*

$$\dot{u} = -\frac{1}{k_d}\left(k_i\left(u - \overline{u}\right) + \left(\dot{I}V - \dot{V}I + V_s\dot{I}\right)\right), \qquad (77)$$

with $k_d > 0$ and $k_i > 0$. Then, the solution (I, V, u) to the closed-loop system asymptotically converges to the desired steady-state $\left(\overline{I}, V^\star, \overline{u}\right)$.

B. Cúk Converter

The average governing dynamic equations of the Cúk converter are the following:

$$-L_1\dot{I}_1 = (1 - u)V_1 - V_s \qquad (78a)$$
$$-L_2\dot{I}_2 = uV_1 + V_2 \qquad (78b)$$
$$C_1\dot{V}_1 = (1 - u)I_1 + uI_2 \qquad (78c)$$
$$C_2\dot{V}_2 = I_2 - GV_2. \qquad (78d)$$

Equivalently, system (78) can be obtained from (8) with $\Gamma_0 = \begin{bmatrix} 1 & 0 \\ 0 & 1 \end{bmatrix}$, $\Gamma_1 = \begin{bmatrix} 0 & 0 \\ 1 & 1 \end{bmatrix}$, $B_0 = B_1 = \begin{bmatrix} 1 & 0 \end{bmatrix}^\top$, $P_R(I) = 0$ and $P_G(V) = \frac{1}{2}GV_2^2$. By using Proposition 2, the following passivity property is established.

Lemma 6 (Passivity property of the Cúk converter). *Let Assumptions 1 and 2 hold. System (78) is passive with respect to the storage function (19) and the port-variables $\dot{u}$ and $y = \dot{V}_1\left(I_2 - I_1\right) - V_1\left(\dot{I}_2 - \dot{I}_1\right)$.*

By virtue of the above passivity property, we can now use the input shaping methodology to design a voltage controller.

Corollary 6 (Input shaping for the Cúk converter). *Let Assumptions 1–3, 5 and 6 hold. Consider system (76) with the dynamic ocntroller*

$$\dot{u} = -\frac{1}{k_d}\left(k_i\left(u - \overline{u}\right) + \dot{V}_1\left(I_2 - I_1\right) - V_1\left(\dot{I}_2 - \dot{I}_1\right)\right), \qquad (79)$$

with $k_d > 0$ and $k_i > 0$. Then, the solution (I, V, u) to the closed-loop system asymptotically converges to the desired steady-state $\left(\overline{I}, V^\star, \overline{u}\right)$.

REFERENCES

[1] D. Jeltsema and J. M. A. Scherpen, "Multidomain modeling of nonlinear networks and systems," *IEEE Control Systems Magazine*, vol. 29, no. 4, pp. 28–59, Aug. 2009.

[2] R. Ortega, A. J. van der Schaft, I. Mareels, and B. Maschke, "Putting energy back in control," *IEEE Control Systems Magazine*, vol. 21, no. 2, pp. 18–33, Apr. 2001.

[3] A. J. van der Schaft, *L2-gain and passivity techniques in nonlinear control*. Springer, 2000.

[4] D. J. Hill and P. J. Moylan, "Dissipative dynamical systems: Basic input-output and state properties," *Journal of the Franklin Institute*, vol. 309, no. 5, pp. 327–357, May 1980.

[5] A. J. van der Schaft and D. Jeltsema, "Port-Hamiltonian systems theory: An introductory overview," *Foundations and Trends in Systems and Control*, vol. 1, no. 2-3, pp. 173–378, 2014.

[6] R. Brayton and J. Moser, "A theory of nonlinear networks. I," *Quarterly of Applied Mathematics*, vol. 22, no. 1, pp. 1–33, 1964.

[7] ——, "A theory of nonlinear networks. II," *Quarterly of applied mathematics*, vol. 22, no. 2, pp. 81–104, 1964.

[8] G. Blankenstein, "Geometric modeling of nonlinear RLC circuits," *IEEE Transactions on Circuits and Systems I: Regular Papers*, vol. 52, no. 2, pp. 396–404, Feb. 2005.

[9] D. Jeltsema and J. M. A. Scherpen, "A power-based perspective in modeling and control of switched power converters [past and present]," *IEEE Industrial Electronics Magazine*, vol. 1, no. 1, pp. 7–54, May 2007.

[10] G. Escobar, A. J. van der Schaft, and R. Ortega, "A Hamiltonian viewpoint in the modeling of switching power converters," *Automatica*, vol. 35, no. 3, pp. 445–452, Mar. 1999.

[11] H. Sira-Ramirez, R. Ortega, and G. Escobar, "Lagrangian modeling of switch regulated DC-to-DC power converters," in *Proceedings of 35th IEEE Conference on Decision and Control*, vol. 4, Dec. 1996, pp. 4492–4497.

[12] J. M. A. Scherpen, D. Jeltsema, and J. Klaassens, "Lagrangian modeling of switching electrical networks," *Systems & Control Letters*, vol. 48, no. 5, pp. 365–374, Apr. 2003.

[13] R. Ortega and E. García-Canseco, "Interconnection and Damping Assignment Passivity-Based Control: A Survey," *European Journal of Control*, vol. 10, no. 5, pp. 432–450, 2004.

[14] E. García-Canseco, D. Jeltsema, R. Ortega, and J. M. A. Scherpen, "Power-based control of physical systems," *Automatica*, vol. 46, no. 1, pp. 127–132, Jan. 2010.

[15] R. Ortega, A. Loría, P. J. Nicklasson, and H. Sira-Ramírez, *Passivity-based Control of Euler-Lagrange Systems*, ser. Communications and Control Engineering. London: Springer London, 1998.

[16] R. Mehra, S. G. Satpute, F. Kazi, and N. Singh, "Control of a class of underactuated mechanical systems obviating matching conditions," *Automatica*, vol. 86, pp. 98–103, Dec. 2017.

[17] M. Zhang, P. Borja, R. Ortega, Z. Liu, and H. Su, "PID passivity-based control of port-Hamiltonian systems," *IEEE Transactions on Automatic Control*, vol. 63, no. 4, pp. 1032–1044, Apr. 2018.

[18] P. Borja, R. Cisneros, and R. Ortega, "A constructive procedure for energy shaping of port-Hamiltonian systems," *Automatica*, vol. 72, pp. 230–234, Oct. 2016.

[19] V. Chinde, K. C. Kosaraju, A. Kelkar, R. Pasumarthy, S. Sarkar, and N. M. Singh, "A passivity-based power-shaping control of building HVAC systems," *Journal of Dynamic Systems, Measurement, and Control*, vol. 139, no. 11, July 2017.

[20] D. Jeltsema and J. M. A. Scherpen, "Tuning of passivity-preserving controllers for switched-mode power converters," *IEEE Transactions on Automatic Control*, vol. 49, no. 8, pp. 1333–1344, Aug. 2004.

[21] H. Khalil, *Nonlinear Systems*, 3rd ed. Prentice Hall, 2002.

[22] R. Pasumarthy, K. C. Kosaraju, and A. Chandrasekar, "On power balancing and stabilization for a class of infinite-dimensional systems," in *21st International Symposium on Mathematical Theory of Networks and Systems, Groningen, The Netherlands*, July 2014.

[23] K. C. Kosaraju, R. Pasumarthy, N. M. Singh, and A. L. Fradkov, "Control using new passivity property with differentiation at both ports," in *Proceedings of the Indian Control Conference (ICC)*, Guwahati, India, Jan. 2017, pp. 7–11.

[24] K. C. Kosaraju, V. Chinde, R. Pasumarthy, A. Kelkar, and N. M. Singh, "Differential passivity like properties for a class of nonlinear systems," in *Proceedings of the American Control Conference (ACC)*, Milwaukee, WI, USA, June 2018, pp. 3621–3625.

[25] D. Jeltsema, R. Ortega, and J. M. A. Scherpen, "On passivity and power-balance inequalities of nonlinear RLC circuits," *IEEE Transactions on Circuits and Systems I: Fundamental Theory and Applications*, vol. 50, no. 9, pp. 1174–1179, Sept. 2003.

[26] J. Zhao and F. Dörfler, "Distributed control and optimization in DC microgrids," *Automatica*, vol. 61, pp. 18 – 26, Nov. 2015.

[27] M. Cucuzzella, R. Lazzari, S. Trip, S. Rosti, C. Sandroni, and A. Ferrara, "Sliding mode voltage control of boost converters in DC microgrids," *Control Engineering Practice*, vol. 73, pp. 161–170, Apr. 2018.

[28] C. De Persis, E. R. Weitenberg, and F. Dörfler, "A power consensus algorithm for DC microgrids," *Automatica*, vol. 89, pp. 364–375, Mar. 2018.

[29] K. Cavanagh, J. A. Belk, and K. Turitsyn, "Transient Stability Guarantees for Ad Hoc DC Microgrids," *IEEE Control Systems Letters*, vol. 2, no. 1, pp. 139–144, Jan. 2018.

[30] S. Trip, M. Cucuzzella, X. Cheng, and J. M. Scherpen, "Distributed averaging control for voltage regulation and current sharing in DC microgrids," *IEEE Control Systems Letters*, vol. 3, no. 1, pp. 174–179, Jan. 2019.

[31] M. Cucuzzella, S. Trip, C. De Persis, X. Cheng, A. Ferrara, and A. J. van der Schaft, "A Robust Consensus Algorithm for Current Sharing and Voltage Regulation in DC Microgrids," *IEEE Transactions on Control Systems Technology*, vol. 27, no. 4, pp. 1583–1595, July 2019.

[32] H. Broer and F. Takens, "Preliminaries of dynamical systems theory," in *Handbook of Dynamical Systems*. Elsevier Science, 2010, vol. 3, ch. 1, pp. 1–42.

[33] A. van der Schaft, "On The Relation Between Port-Hamiltonian And Gradient Systems," *IFAC Proceedings Volumes*, vol. 44, no. 1, pp. 3321–3326, 2011, 18th IFAC World Congress.

[34] K. C. Kosaraju, R. Pasumarthy, and D. Jeltsema, "Modeling and boundary control of infinite dimensional systems in the brayton–moser framework," *IMA Journal of Mathematical Control and Information*, vol. 36, no. 2, pp. 485–513, 2019.

[35] D. Jeltsema, J. Clemente-Gallardo, R. Ortega, J. M. A. Scherpen, and J. B. Klaassens, "Brayton-moser equations and new passivity properties for nonlinear electromechanical systems," *Proc. 8th Mechatronics Forum International Conference*, pp. 979–988, June 2002.

[36] A. Favache and D. Dochain, "Power-shaping control of reaction systems: The CSTR case," *Automatica*, vol. 46, no. 11, pp. 1877–1883, 2010.

[37] M. Guay and N. Hudon, "Stabilization of nonlinear systems via potential-based realization," *IEEE Transactions on Automatic Control*, vol. 61, no. 4, pp. 1075–1080, Apr. 2016.

[38] F. Forni, R. Sepulchre, and A. J. van der Schaft, "On differential passivity of physical systems," in *Proceedings of the 52nd IEEE Conference on Decision and Control (CDC)*, Florence, Italy, Dec. 2013, pp. 6580–6585.

[39] M. Cucuzzella, R. Lazzari, Y. Kawano, K. Kosaraju, and J. M. A. Scherpen, "Robust Passivity-Based Control of Boost Converters in DC Microgrids," in *Proceedings of the 58th IEEE Conference on Decision and Control (CDC)*, Nice, France, Dec. 2019, pp. 8435–8440.

[40] M. Cucuzzella, K. C. Kosaraju, and J. M. A. Scherpen, "Voltage control of DC networks: robustness for unknown ZIP-loads," *arXiv preprint: 1907.09973*, July 2019.

[41] M. Cucuzzella, K. C. Kosaraju, and J. M. A. Scherpen, "Distributed Passivity-Based Control of DC Microgrids," in *2019 American Control Conference (ACC)*, July 2019, pp. 652–657.

[42] K. C. Kosaraju, Y. Kawano, and J. M. A. Scherpen, "Krasovskii's passivity," *IFAC-PapersOnLine*, vol. 52, no. 16, pp. 466–471, 2019.

[43] Y. Kawano, K. C. Kosaraju, and J. M. A. Scherpen, "Krasovskii and shifted passivity based control," *arXiv:1907.07420*, 2019.

Krishna Chaitanya Kosaraju received the Bachelor degree in Electronics and Instrumentation from Birla Institute of Technology and Science - Pilani, 2010. He received his Master degree in Control and Instrumentation and the Ph.D. degree in Electrical Engineering from Indian Institute of Technology - Madras, in 2013 and 2018, respectively. Currently he is a Postdoc at the University of Notre Dame, under the supervision of Professor Vijay Gupta. From April 2018 to December 2019, he was a Postdoc at the University of Groningen, under the supervision of Professor J.M.A. Scherpen. His research activities are mainly in the area of nonlinear control theory, passivity based control and optimization theory with application to power networks, Building systems and Reinforcement learning.

Michele Cucuzzella received the Bachelor degree (with highest honor) in Industrial Engineering, the Master degree (with highest honor) in Electrical Engineering and the Ph.D. degree (with highest honor) in Electronics, Computer Science and Electrical Engineering from the University of Pavia, in 2012, 2014 and 2018, respectively. From April to June 2016, and from February to March 2017 he was with the Johann Bernoulli Institute for Mathematics and Computer Science at the University of Groningen, under the supervision of Professor A. van der Schaft. Currently he is a Postdoc at the University of Groningen, under the supervision of Professor J. Scherpen. His research activities are mainly in the area of nonlinear control with application to power networks. He is IEEE member since 2016 and, currently, he is Associate Editor for the European Control Conference. He received the IEEE Italy Section Award for the best Ph.D. thesis on new technological challenges in energy and industry, and the SIDRA Award for the best Ph.D. thesis in the field of systems and control engineering.

Jacquelien M. A. Scherpen received the M.Sc. and Ph.D. degrees in applied mathematics from the University of Twente, Enschede, The Netherlands, in 1990 and 1994, respectively. She was with Delft University of Technology, The Netherlands, from 1994 to 2006. Since September 2006, she has been a Professor with the University of Groningen, at the Engineering and Technology institute Groningen (ENTEG) of the Faculty of Science and Engineering, Groningen, The Netherlands. She is currently scientific director of ENTEG (until 2019), and of the Groningen Engineering Center. She has held visiting research positions at The University of Tokyo, Japan, Université de Compiegne, SUPELEC, Gif-sur-Yvette, France, and the Old Dominion University, Norfolk, VA, USA. Her current research interests include nonlinear model reduction methods, nonlinear control methods, modeling and control of physical systems with applications to electrical circuits, electromechanical systems and mechanical systems, and distributed optimal control applications to smart grids. Prof. Scherpen has been an Associate Editor of the IEEE TRANSACTIONS ON AUTOMATIC CONTROL, the International Journal of Robust and Nonlinear Control (IJRNC), and the IMA Journal of Mathematical Control and Information. She is on the Editorial Board of the IJRNC.

Ramkrishna Pasumarthy obtained his PhD in systems and control from the University of Twente, The Netherlands. He is currently with the Indian Institute of Technology Madras, India and is also associated with the Robert Bosch Center for data sciences and artificial intelligence at IIT Madras. His research interests are mainly in the area of modeling and control of complex physical systems, together with identification and control of (cloud) computing systems and data analytics for power, traffic, cloud and brain networks.